Dative and Di−σ Binding States of Pyridine on Si(100) and Their Thermal Stability

Feng Tao,[†] Ming Hua Qiao,[‡] Zhong Hai Wang,[†] and Guo Qin Xu*,[†]

Department of Chemistry, National University of Singapore, 10 Kent Ridge, Singapore 119260, and Department of Chemistry, Fudan University, Shanghai, P.R. China 200433

Received: February 27, 2003

The chemical binding of pyridine on Si(100) has been studied using thermal desorption spectroscopy (TDS), X-ray phototelectron spectroscopy (XPS), high-resolution electron energy loss spectroscopy (HREELS), and DFT theoretical calculations. XPS results show two chemisorption states of pyridine with N 1s binding energies at 398.8 and 401.8 eV, attributable to the [4+2]-like cycloadduct with two σ-linkages of Si−N[1] and Si−C[4], and the dative-bonded pyridine through the lone pair electrons of its N atom, respectively. These observations were further confirmed in our vibrational studies. The formation of a dative bond between pyridine and Si(100) demonstrates a new approach for the chemical attachment of unsaturated organic molecules on the Si surface. The 1,4-dihydropyridine-like cycloadduct formed at 350 K can be considered as a template for further modification and functionalization of Si surfaces or as an intermediate for syntheses in a vacuum.

I. Introduction

Si(100) is a particularly important semiconductor surface because of its extensive technological relevance.[1,2] In its (2 × 1) reconstructed structure, adjacent Si atoms pair into dimers, shown in Figure 1a. The bonding within a surface dimer can be formally described in the terms of a σ bond coupled with a π bond,[3,4] analogous to the C=C double bonds of alkenes, suggesting a possible similarity of chemical reactivities between them. Because of the large Si−Si distance and bending back-bonds that connect the surface dimer with the bulk atoms, the π bond in a Si=Si dimer is quite weak. In fact, the Si=Si dimer might be regarded as a di-radical[5] as schematically presented in Figure 1b. About 20 years ago, Chadi predicted that the asymmetric configuration was energetically favorable over the symmetric dimer on Si(100).[6] A great number of subsequent theoretical[7,8] and experimental[9−11] studies confirmed the existence of buckling Si=Si dimer at low temperature. The dimer buckling is accompanied by a charge transfer from the buckled-down atom to the buckled-up one. Its scheme is shown in Figure 1c. However, at room temperature, owing to the rapid dynamical flipping between the two alternative buckling orientations, the Si=Si dimers do not generally display asymmetry, as described in Figure 1d. Within a buckling dimer, the transfer of electron density causes the buckled-down Si atom to be electron-deficient, but electron-rich for the buckled-up one, indicating ionic character.[6] These Si atoms may possibly act as either electron acceptors or donors through the formation of dative bonds with molecules. Therefore, the unique bonding motifs of Si=Si dimers as described above may suggest special attachment strategies and multiple chemical binding states for unsaturated organic molecules, including the dative and covalent attachment schemes.

Previous studies showed that unsaturated organic molecules can be covalently bonded to Si(100) through [2+2]-like or/and [4+2]-like cycloadditions to form di−σ or tetra−σ linkages.[1,12−38]

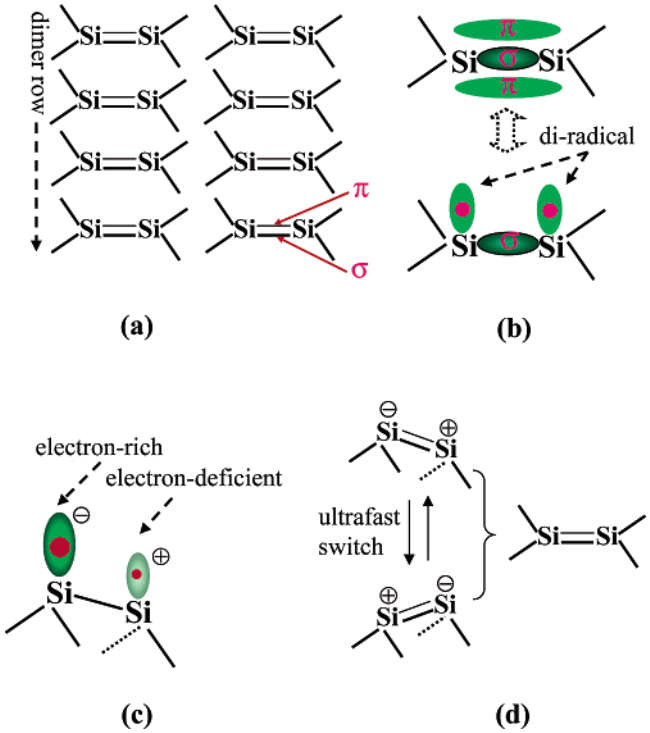

Figure 1. Schematic presentation of the Si(100) surface structure at low temperature and room temperature. (a) (2 × 1) surface structure of Si(100); (b) spatial and electronic structure of Si=Si dimer; (c) electronic structure of buckling Si=Si dimer at low temperature; (d) thermal flopping of Si=Si dimer and symmetric Si=Si dimer at room temperature.

The attachment of unsaturated organic molecules through the dative bond has not been demonstrated. However, the ability of Si(100) to act as an electron acceptor was implied in the interaction of containing N molecules, including NH_3[39,40] and $C_6H_5NH_2$[41−44] with Si surface. Theoretical calculations suggested that the interaction between the lone pair electrons on nitrogen atom and one end of a Si=Si dimer via a transient dative bond weakens the N−H bond, subsequently causing the

* To whom correspondence should be addressed. E-mail: chmxugq@nus.edu.sg. Fax: (65)-6779-1691.
[†] National University of Singapore.
[‡] Fudan University.

10.1021/jp030259e CCC: $25.00
Published on Web 06/10/2003

dissociative adsorption.[39,40] A similar mechanism was also proposed for other NH-containing molecules.[41−44] These experimental results and theoretical studies showed that the formation of the dative bond in NH-containing molecules is competitive, but the dissociative adsorption via the cleavage of the N−H bond is thermodynamically more favorable. Indeed, a similar dative-bonding scheme was evidenced in recent studies of amines adsorption on Si(100).[45−48]

To further understand the reaction selectivity and competitiveness between the covalent cycloaddition and the dative bonding, we have studied a series of unsaturated organic molecules containing C≡N or C−N bonds. For molecules containing C≡N on Si(100), the covalent attachment occurs only through the [2+2]-like or [4+2]-like cycloaddition reaction.[14−20] In the recent studies of pyrrole/Si(100)[41] and *N*-methylpyrrole/Si(100),[49] no evidence for the dative bond was found, possibly because of the participation of the lone pair electrons of the nitrogen atom in the formation of the aromatic ring. Pyridine is a six-membered heteroatomic aromatic molecule. Each of the constituent C and N atoms contributes one electron to form a conjugated π system, leaving one lone pair of electrons on its nitrogen atom. In view of the high reactivity of aromatic molecules on Si(100) through [4+2]-like or/and [2+2]-like cycloaddition pathways,[50−54] pyridine could be expected to react with Si(100) through the established [4+2]-like or/and [2+2]-like cycloaddition, forming two Si−C or/and Si−N sigma linkages. In addition, the lone-pair electrons localized on the nitrogen atom may possibly act as an electron donor to form the dative bond with the electron-deficient buckled-down Si atom in a Si═Si dimer. Thus, the coexistence of the dative-bonded addition product and sigma-bonded cycloadduct for pyridine on Si(100) may be possible.

In this paper, the attachment chemistry of pyridine on Si(100) was studied. XPS provides information on chemical shifts of the N 1s core level. HREELS was used to characterize the vibrational properties of pyridine on Si(100). DFT calculations (*p*BP/DN** in Spartan 5.1) were commanded to optimize possible chemisorption geometries and calculate their adsorption energies. Our experimental results together with DFT calculations show that (a) pyridine chemically binds to Si(100) through dative-bonding and [4+2]-like addition reaction in a temperature range of 110−350 K; (b) the Si:N dative-bonded pyridine is thermally sensitive, possibly converting to covalent di−σ bonded cycloadduct with the increase of temperature. The two surface intermediates, the dative-bonded pyridine and 1,4-dihydropyridine-like structure formed through [4+2]-like cycloaddition, may be used as precursors for further modification and functionalization of silicon surface and syntheses in a vacuum.

II. Experimental Section

The experiments were preformed in two ultrahigh vacuum (UHV) systems with a base pressure lower than 2×10^{-10} Torr. Photoemission studies were carried out in one chamber equipped with an X-ray source and a concentric hemispherical energy analyzer (CLAM2, VG). XPS spectra were collected using Mg Kα radiation ($h\nu = 1253.6$ eV) and 10 eV pass energy. For the photoemission studies, the binding energy is referenced to the peak maximum of the Si 2p line (99.3 eV calibrated to Au $4f_{7/2}$[55]) of the Si(100) substrate with a routine full width at half-maximum (fwhm) of less than 1.2 eV. XPS spectra were analyzed using standard curve-fitting procedures in software VGX900 [56] (VG Microtech, U.K.).

Another UHV chamber is equipped with a high-resolution electron energy loss spectrometer (HREELS, LK-2000-14R).

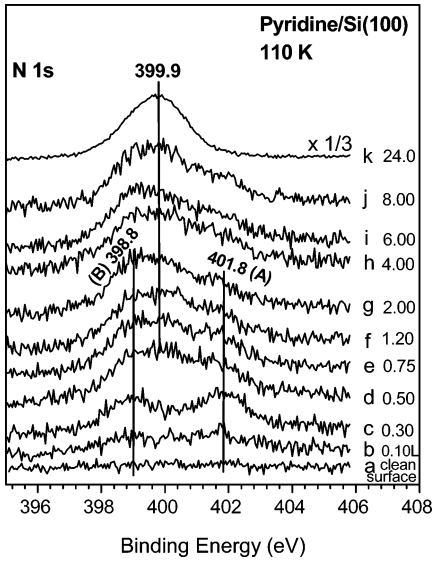

Figure 2. N 1s XPS for pyridine adsorbed on Si(100) as a function of exposure at 110 K.

HREELS measurements were taken in a specular geometry. The electron beam with an energy of 5.0 eV impinges on the surface at an incident angle of 60° with respect to the surface normal. A typical instrument resolution of ∼5 meV (∼40 cm^{-1}) is achieved.

The Si(100) samples were cut from *n*-type phosphorus-doped silicon wafer (99.999%, 1−30 Ω cm, Goodfellow) and were rinsed. The details of sample mounting procedures were described elsewhere.[16,19] After degassing overnight in UHV systems with a pressure lower than 4×10^{-10} Torr, clean Si(100) samples were prepared by Ar^+ ion bombardments (1 keV, 30 min, ∼5−10 μA cm^{-2}) and final annealing at 1300 K for ∼20 min to form the 2×1 reconstruction. The cleanliness of the samples was confirmed with XPS and HREELS.

Pyridine (99%, Aldrich) and pyridine-2-d_1 (98.2 atom % D, 99.9% purity, C/D/N Isotopes, Inc.) were further purified through at least five freeze−pump−thaw cycles before being dosed onto the clean Si(100) surface at 110 K. Dosing was preformed by backfilling the chamber, and the exposures were reported in Langmuirs (1 langmuir = 10^{-6} Torr s) without the calibration of ion gauge sensitivity.

III. Results and Discussion

III.A. X-ray Photoelectron Spectroscopy. Figure 2 shows the N 1s XPS spectra of pyridine adsorbed on Si(100) at 110 K as a function of exposure. Two photoemission features can be identified at 401.8 and 398.8 eV at the exposures of ∼0.1−2.0 langmuir. Their binding energies do not show observable chemical shifts with the increase of exposure. Further increasing in exposure leads to the appearance of an N 1s peak at 399.9 eV which becomes dominant at the exposure higher than 8.0 langmuir. For the exposure of ∼24 langmuir, the photoemission intensities at 398.8 and 401.8 eV are completely attenuated and only the N 1s peak at 399.9 eV can be observed.

The two photoemission features at 398.8 and 401.8 eV for N 1s core level taken after initial dose can be ascribed to two distinctly different chemisorption states. The peak at 399.9 eV dominant at high exposures is attributable to physisorbed pyridine molecules, in line with the studies of pyridine on Ni(110).[57] Because TDS studies show that physisorbed molecules completely desorb from the surface at 170 K (starting from 130 K), exposing pyridine onto the surface at an adsorption

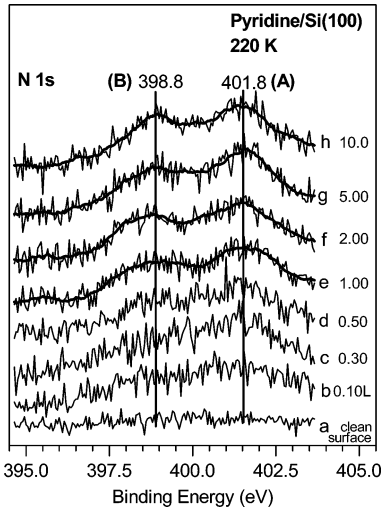

Figure 3. N 1s XPS for pyridine adsorbed on Si(100) as a function of exposure at 220 K.

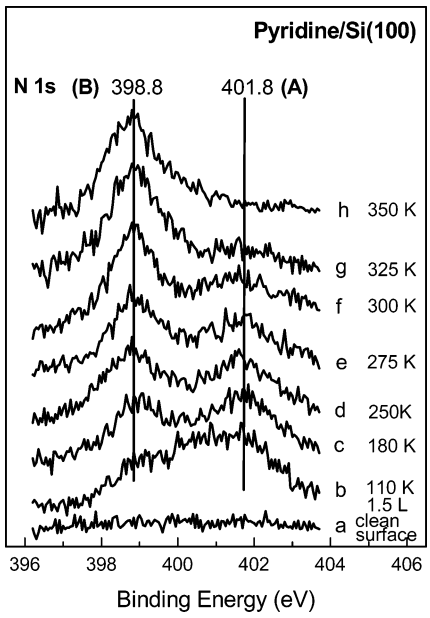

Figure 4. N 1s XPS for pyridine adsorbed on Si(100) as a function of temperature (110−350 K).

temperature higher than 170 K will result in pure chemisorbed species. Figure 3 shows the N 1s spectra collected after pyridine adsorption on Si(100) at 220 K. Only two N 1s peaks at 398.8 and 401.8 eV, similar to the photoemission features in Figure 2, parts b and c, are detected, confirming their chemisorption natures. However, both of them nearly reach saturation at the exposure of 2.0 langmuir at 220 K. The saturated ratio of N 1s peak-area at 398.8 (state B) to that at 401.8 eV (state A) is found to be ∼4:5. It is also noted that high exposures at 220 K do not result in physisorption features at 399.9 eV observed for adsorption at 110 K, consistent with the TDS results (not shown).

To investigate the possible conversion between the two chemisorption states, XPS studies were carried out as a function of sample temperature between 110 and 350 K (Figure 4). It can be seen that two peaks at 398.8 and 401.8 eV with an area-ratio of ∼3:4 are coexistent at 180 K. An increase in temperature leads to the gradual decrease in the intensity of peak at 401.8 eV but some growth of the 398.8 eV peak. At 350 K, only the peak at 398.8 eV can be observed. It is also noted that there are no detectable chemical shifts for these two peaks during

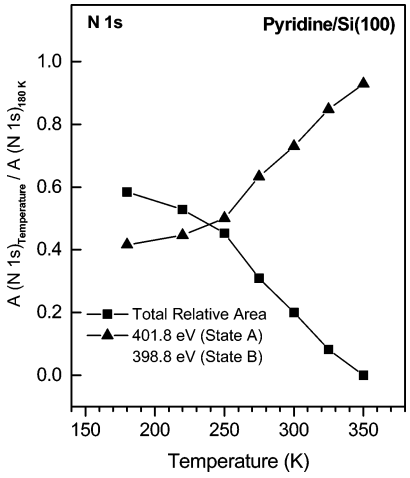

Figure 5. Relative intensities [referenced to the total intensity of two N 1s peaks at 180 K, $A(\mathrm{N\ 1s})_{\mathrm{temperature}}/A(\mathrm{N\ 1s})_{180\mathrm{K}}$] of N 1s peaks at 401.8 and 398.8 eV as a function of temperature (180−350 K).

the thermal annealing process in the range of 180−350 K, indicating no new species formed. The changes in the relative peak areas for N 1s at 401.8 and 398.8 eV and their sum as a function of sample temperature are shown in Figure 5. It suggests the trend of decreasing in N 1s at 401.8 eV accompanied with the increase of the peak at 398.8 eV as a function of sample temperature. These observations suggest that some chemisorbed molecules of state A (N 1s 401.8 eV) possibly convert into chemisorption state B (N 1s 398.8 eV) when the sample is heated from 180 to 350 K.

Two chemisorption states, denoted as states A (N 1s 401.8 eV) and B (N 1s 398.8 eV), have been observed for pyridine on Si(100). XPS studies show that state A represents ∼54% of chemisorbed molecules at 220 K. N 1s core level of state A at 401.8 eV is ∼3.0 eV higher than the typical values of 398.5−399.3 eV for pyrrole,[58] pyrroilidine,[59] NH_3,[60−62] and aniline[41,42] dissociatively chemisorbed on Si(100) and pyridine di−σ bonded to Si(100) through cycloaddition reaction. This N 1s binding energy of state A is also ∼2 eV higher than the value of physisorbed pyridine (Figure 2). The unusually high binding energy suggests a critically electron-deficient environment around the N atom. In fact, previous studies showed that the N 1s core levels for $[(CH_3)_4N]^+Cl^-$ [63] and $[(CH_3)_4N]^+Br^-$ [64,65] are 401.6 and 402.5 eV, respectively. Obviously, the N 1s core level for state A is comparable to the values of 401.6 and 402.5 eV for the two ammonium salts. Thus, it is reasonable to deduce that the unusually high value of 401.8 eV observed for state A is possibly resulted from the significant transfer of electron density from the N atom of pyridine to one Si atom of Si═Si dimer through the formation of a ionic dative bond, by which dative-bonded pyridine may possibly act as a molecular cation. The nature of state B will be demonstrated in the following vibrational studies.

III.B. High-Resolution Electron Energy Loss Spectroscopy. To understand the binding configurations of the chemisorption states, vibrational studies were conducted. Figure 6 shows the HREELS spectra of physisorbed pyridine and chemisorbed molecules on Si(100) as a function of exposure at 110 K. The vibrational frequencies and assignments for physisorbed molecules are tabulated in Table 1. This table clearly shows that the vibrational features of physiosrbed pyridine are in excellent agreement with the IR spectra of liquid and gaseous pyridine[66,67] as well as the previous HREELS studies of pyridine physisorbed on transition metals.[68] Among these vibrational

TABLE 1: Assignments of HREELS Spectra of Physisorbed Pyridine at 110 K and Di−σ Bonded Molecules at 350 K on Si(100)[a]

mode	vibrational character	liquid pyridine[66,67]	physisorbed pyridine	vibrational character	liquid 1,4-cyclohexadiene[70−72]	di−σ bonded pyridine (350 K)
ν_{22}	out of plane	374	391	=CH stretch	3032, 3019	3045
ν_{27}	out of plane	405		$-CH_2$ stretch	2877, 2875, 2825, 2822	2895
ν_{10}	in plane (ring mode)	605		C=C stretch	1680, 1639	1630
ν_{19}	in plane (ring mode)	652		-CH_2 scissors	1430, 1426	1419, 1460
ν_{26}	out of plane	700		-CH_2 wag	1358	1352
ν_{25}	out of plane	749	745	-CH_2 twist	1100	1096
ν_{21}	out of plane	886	885	=Ch in plane bend	1197, 1193, 1159, 1035	1210, 1210[a], 1165,1050
ν_{24}	out of plane	882		=CH out of plane bend	1000, 985, 706, 632	964, 756
ν_{23}	out of plane	942		-CH_2 rock	956	964[a]
ν_{20}	out of plane	981	990	C−C(ring) stretch	1405, 1377, 956	1419[a], 1352[a], 964[a]
ν_9	in plane (ring mode)	992		Ring motion	887, 854, 574, 530, 404, 250, 210	870
ν_8	in plane (ring mode)	1030	1020			
ν_7	in plane	1068	1058	Si−C stretch		615
ν_{18}	in plane	1085		Si−N stretch		495
ν_{17}	in plane	1148	1142			
ν_6	in plane	1218	1220			
ν_{16}	in plane	1212				
ν_{15}	in plane	1375	1365			
ν_{14}	in plane (ring mode)	1439	1428			
ν_5	in plane (ring mode)	1482	1492			
ν_{13}	in plane (ring mode)	1572	1580			
ν_4	in plane (ring mode)	1583				
ν_3, ν_{12}	C−H stretching	3036(2)	3065			
ν_1, ν_2	C−H stretching	3054(2)				
ν_{11}	C−H stretching	3083				

[a] All frequencies are in cm^{-1}.

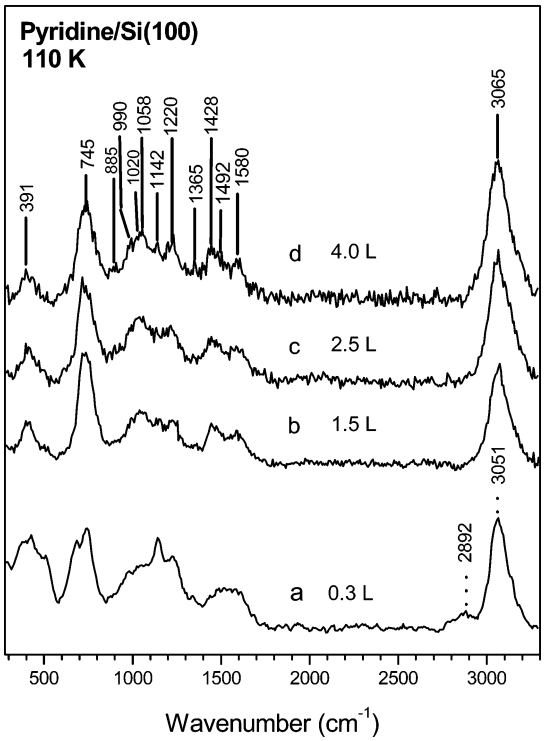

Figure 6. HREELS spectra as a function of pyridine exposure on Si(100) at 110 K.

signatures, the single peak at 3065 cm^{-1} is assigned to C^{sp2}−H stretching modes.

At low exposures (Figure 6a), the vibrational features are mainly contributed from chemisorbed molecules, evidenced by the XPS results at 0.30 langmuir and 110 K (Figure 2c). It can be seen that this spectrum (Figure 6a) displays some similarities to physisorbed molecules (Figure 6b−d). Compared to physisorbed molecules, there is a significant difference found for C−H stretching modes. For chemisorbed molecules (Figure 6a), the C−H stretching presents as a doublet at 3051 and 2892 cm^{-1} with an intensity ratio of ~9:1.

Previous studies showed that benzene can be covalently attached on Si(100)[38] and Si(111)-7 × 7[69] through the formation of two new Si−C σ-bond linkages, evidenced by the doublet at ~3050 and ~2908 cm^{-1} assigned to C^{sp2}−H and C^{sp3}−H stretching modes, respectively. Therefore, the two separated peaks at ~3051 and ~2892 cm^{-1} in Figure 6a corresponding to the ν(C−H) for chemisorbed pyridine demonstrate the existence of sp^3 C atom due to the rehybridization of one or more sp^2 C atoms. This shows the formation of new Si−C sigma bonds by covalent attachment mode via cycloaddition mechanism in one or two chemisorption states, similar to unsaturated hydrocarbons molecularly chemisorbed on Si(100).[38,51−54] Because of the coexistence of two states (A and B) at low exposure of 0.3 langmuir and 110 K, the HREELS spectra of chemisorbed pyridine (Figure 6a) are rather complicated for detailed assignment.

Figure 7 presents the vibrational signatures of pyridine chemisorbed on Si(100) upon annealing the sample to the indicated temperatures. The spectrum (Figure 7a) obtained after exposing pyridine of 1.5 langmuir at 110 K mainly presents the vibrational features of physisorbed molecules. Annealing the multilayer pyridine covered surface to ≥170 K causes the complete desorption of physisorbed molecules, leaving only the chemisorbed pyridine on the surface. Thus, Figure 7c−f shows the changes of vibrational features of chemisorption states as a function of surface temperature, similar to the thermal evolution of N 1s core level for chemisorbed pyridine (Figure 4c−h). Compared to the feature at ~3045 cm^{-1}, the relative intensity at ~2895 cm^{-1} is evidenced to increase with the sample temperature. In addition, the vibrational features of Si−C(N) stretching modes[24,58] at 615 (495) cm^{-1} become intensified at higher temperatures. Significant changes occur in the spectrum

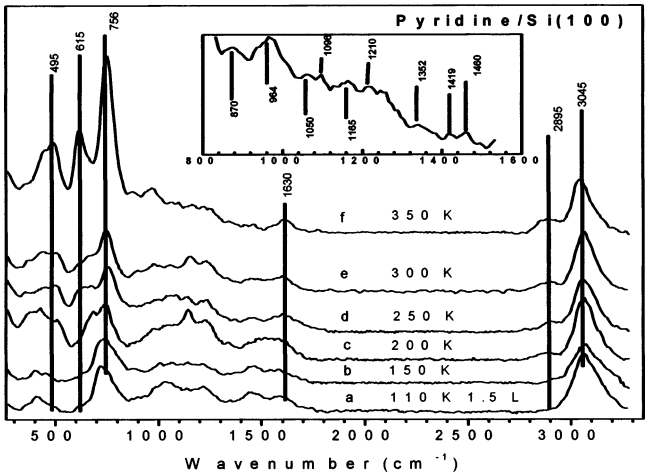

Figure 7. HREELS spectra for pyridine adsorbed on Si(100) as a function of temperature (110−350 K). The insert is the enlargement of Figure 7f at 830−1530 cm^{-1}.

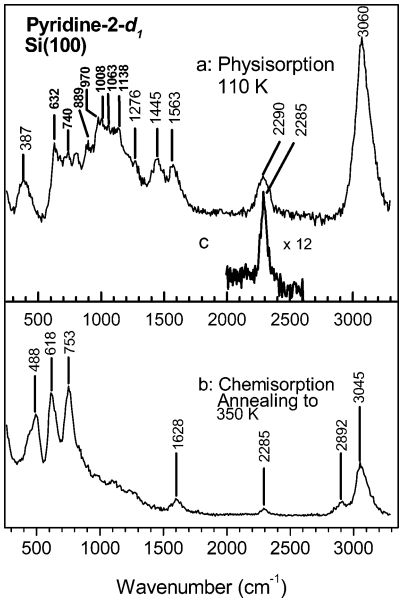

Figure 8. HREELS spectra for physisorbed pyridine-2-d_1 (a) and chemisorbed molecules (b) on Si(100). Figure 8c is the enlargement of Figure 8b at the region of 2000−2500 cm^{-1}.

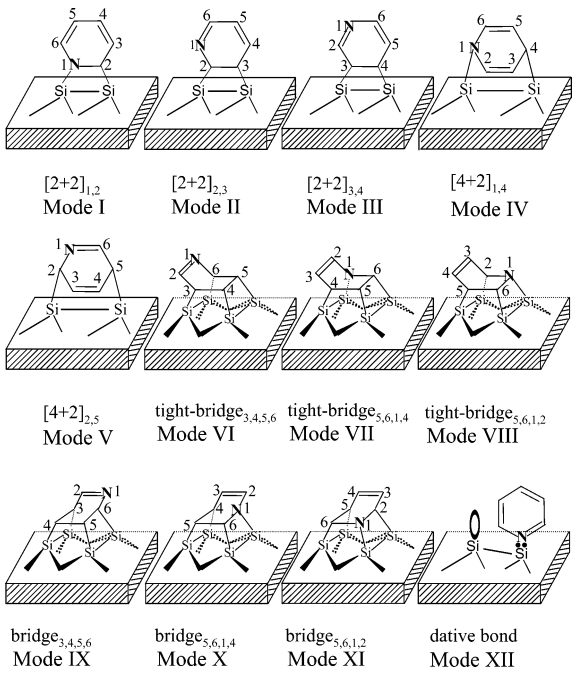

Figure 9. Schemes of possible di−σ and tetra−σ as well as dative-bonded binding modes for pyridine chemically attached to Si(100).

of chemisorbed pyridine at 350 K (Figure 7f), consistent with our XPS studies (Figure 4). Thus, the vibrational features presented in Figure 7f are contributed solely from the chemisorption state B. The observation of Si−C (615 cm^{-1}) and Si−N (495 cm^{-1}) together with the coexistence of C^{sp2}−H (3045 cm^{-1}) and C^{sp3}−H (2895 cm^{-1}) stretching modes seems to suggest the formation of di−σ bonded pyridine. The detailed assignments of vibrational signatures of di−σ bonded pyridine on Si(100) at 350 K are listed in Table 1, together with the vibrational frequencies of liquid 1,4-cyclohexadiene.[70−72] The close resemblance between chemisorbed pyridine at 350 K and 1,4-cyclohexadiene further supports the σ-bonding nature of state B and implies the formation of a [4+2]-like cycloadduct through the N atom and its opposite C atom. The absence of Si−H peak in vibrational spectra for chemisorbed pyridine on Si(100) at temperatures ≤350 K clearly indicates the molecular adsorption nature without the cleavage of C−H bonds.

To further identify the cycloaddition mechanism and binding configuration for the chemisorption state B of pyridine on Si(100), pyridine-2-d_1 adsorption was also studied. Figure 8, parts a and b, is the vibrational features of physisorbed pyridine-2-d_1 at 110 K and chemisorbed molecules at 350 K (State B) on Si(100), respectively. The enlargement of Figure 8b at the region of 2000−2500 cm^{-1} is presented in Figure 8c. In these vibrational signatures of physisorbed molecules, the peaks at 3060 and 2290 cm^{-1} are ascribed to C^{sp2}−H and C^{sp2}−D stretching modes, respectively. The vibrational features of σ-bonded pyridine-2-d_1 (state B) obtained by annealing the sample to 350 K to completely convert state A to B, however, are significantly different. Losses at 488, 618, 753, 1628, 2285, 2892, and 3045 cm^{-1} can be readily resolved. Compared to physisorbed pyridine-2-d_1 on Si(100), upon chemisorption (a) the peak for C−H stretching becomes a doublet, suggesting the rehybridization of one or more C atoms from sp^2 to sp^3, and (b) the peak attributed to the C^{sp2}−D stretching mode does not display observable shift, showing that C^2 and C^6 atoms do not directly take part in the cycloaddition reaction with the Si surface. In addition, the concurrent participation of C and N atoms in binding with the surface Si atoms is further confirmed by the observation of peaks for Si−C and Si−N stretching modes[24,25] at 618 and 488, respectively. The above results unambiguously rule out the possibility of the [2+2]-like cycloaddition reaction occurring through both N^1 and C^2 or both N^1 and C,[6] but consistent with the [4+2]-like cycloaddition involving both N^1 and C^4. The rehybridization of N atom from sp^2 into sp^3 is expected to result in significant changes in its electronic structures, consistent with a chemical downshift of ∼1.1 eV for the N 1s core level compared to physisorbed molecules. Therefore, the studies on the vibrational and electronic properties show that the chemisorption state B is formed through the [4+2]-like addition reaction involving both N^1 and C^4 atoms.

III.C. DFT Calculations. If the concept of covalent *di-σ* binding modes is considered, there are five possible configurations: three [2+2]-like cycloadducts (modes I, II, and III of Figure 9) and two [4+2]-like addition products (modes IV and V of Figure 9). There are also six possible addition products covalently linked to Si(100) by four Si−C(N) σ bonds (modes VI, VII, VIII, IX, X, and XI of Figure 9) if including the tetra−σ binding modes, similar to benzene on Si(100). Moreover,

TABLE 2: Adsorption Energies of All Possible Binding Configurations for Pyridine on Si(100)[a]

mode in Figure 9	I	II	III	IV	V	VI	VII	VIII	IX	X	XI	XII
binding mechanism	[2+2]	[2+2]	[2+2]	[4+2]	[4+2]	tight-bridge	tight-bridge	tight-bridge	bridge	bridge	bridge	dative bond
adsorption energy	18.0	11.9	12.7	25.5	30.4	26.4	30.2	36.2	31.0	32.0	24.6	26.9

[a] All energies are in kcal mol^{-1}.

pyridine may react with Si(100) through the formation of Si:N dative bond (mode XII of Figure 9). Our DFT modeling focuses on the geometry optimizations and the calculations of total energies for the twelve possible binding modes to aid the understanding of attachment mechanisms revealed by the experimental results.

For covalent di−σ binding configurations (modes I−V) involving only one Si═Si dimer, we performed DFT calculations for a pyridine molecule adsorbed onto a 9-atom Si cluster (Si_9H_9) using Spartan 5.1.[73] This 9-atom Si cluster with one exposed Si═Si dimer was successfully used in several previous studies of 1,3-cyclohexadiene and 3-butadiene.[27,74] It was also used as the mother cluster in our modeling of the dative-bonded pyridine on Si(100) (mode XII of Figure 9). To model the "tetra−σ" geometries through the aromatic ring (modes VI, VII, VIII, IX, X, and XI of Figure 9), a larger cluster $Si_{16}H_{16}$ with two adjacent Si═Si dimers in the same dimer row was constructed, similar to these successfully employed for the study of benzene on Si(100).[21,75−78] All calculations were preformed using perturbative Beck−Perdew functional (pBP86) in conjugation with a basis set of DN** (comparable 6-31 G**).[73] Geometric optimizations were conducted under SPARTAN default criteria. The calculated adsorption energies of pyridine-bonded clusters corresponding to binding modes I−XII are listed in Table 2. Our energy values of 24−37 kcal mol^{-1} for "tetra−σ" bonded pyridine are comparable to those of benzene in the earlier calculations.[76] Table 2 shows that adsorption energies for the [2+2]-like cycloadducts (modes I, II, and III) are lower than those of [4+2]-like addition products (modes IV and V) and adsorption products formed from "tetra−σ" cycloadditions (modes VI, VII, VIII, IX, X, and XI). In the vibrational studies of σ-bonded pyridine-2-d_1 (state B), we found that the C^2 and C^6 atoms of pyridine do not directly take part in the cycloaddition reaction with the Si surface. Because all of the "tetra−σ" binding configurations should involve at least one C^2 or C^6 atom, their occurrence can be readily ruled out based on our experimental results of pyridine-2-d_1 (Figure 8). Although "tetra−σ" binding configurations have a slightly larger adsorption energy compared to [4+2]-like cycloadducts, a higher transition state may exist in the formation of four Si−C(N) σ linkages. Notably, the adsorption energy of the dative-bonded product (mode XII) is comparable to that of the [4+2]-like addition products (modes IV and V), which suggests the possibility of coexistence of dative-bonded adduct and [4+2]-like cycloadduct, consistent with the HREELS and XPS experimental results.

IV. Conclusions

Experimental results and DFT calculations show that pyridine molecules interact with Si(100) through both Si:N dative bonding and the [4+2]-like cycloaddition between the N^1 and C^4 atoms of the pyridine molecule with a Si═Si dimer, forming pyridine-like and 1,4-dihydropyridine-like adducts, respectively. The coexistence of dative-bonded pyridine and *di*-σ bonded molecules are schematically presented in Figure 10. The dative bonding mode between unsaturated organic molecules and Si surface may possibly establish a new strategy for the fabrication of organic molecular architectures on Si surfaces. The formed

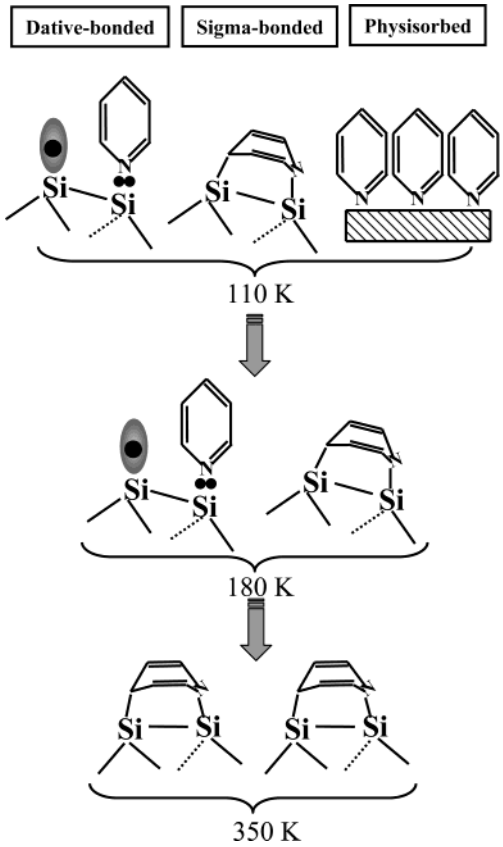

Figure 10. Schematic description of the coexistence of dative-bonded pyridine and di−σ bonded molecules on Si(100).

di−σ bonded product containing two unconjugated C═C double bonds is possibly employed as an intermediate for syntheses in a vacuum via typical vinyl reactions including addition, cyanoethylation, and polymerization, or as a precursor for further modification and functionalization of Si surfaces.

References and Notes

(1) Yates, J. T., Jr. *Science* **1998**, *279*, 335.
(2) Lopinski, G. P.; Moffatt, D.; Wayner, D. D. M.; Wolkow, R. A. *Nature* **1998**, *392*, 909.
(3) Grooks, R. M.; Ticco, A. J. *Acc. Chem. Res.* **1998**, *31*, 219.
(4) Schlier, R. E.; Farnsworth, H. E. *J. Chem. Phys.* **1959**, *30*, 917.
(5) Redondo, A.; Goddard, W. A. *J. Vac. Sci. Technol.* **1982**, *21*, 314.
(6) Chadi, D. J. *Phys. Rev. Lett.* **1979**, *43*, 43.
(7) Paulus, B. *Surf. Sci.* **1998**, *408*, 195.
(8) Shoemaker, J.; Burggraf, L. W.; Gordon, M. S. *J. Chem. Phys.* **2000**, *112*, 2994.
(9) Uhrberg, R. I. G.; Hansson, G. V.; Nicholls, J. M.; Flodstrom, S. A. *Phys. Rev. B* **1981**, *24*, 4684.
(10) Hamers, R. J.; Kohler, U. K. *J. Vac. Sci. Technol. A* **1989**, *7*, 2854.
(11) Hamers, R. J.; Wang, Y. J. *Chem. Rev.* **1996**, *96*, 1261.
(12) Waltenberg, H. N.; Yates, J. T., Jr. *Chem. Rev.* **1995**, *95*, 1589.
(13) Wolkow, R. A. *Annu. Rev. Phys. Chem.* **1999**, *50*, 413.
(14) Tao, F.; Sim, W. S.; Xu, G. Q.; Qiao, M. H. *J. Am. Chem. Soc.* **2001**, *123*, 9397.
(15) Tao, F.; Chen, X. F.; Wang, Z. H.; Xu, G. Q. *J. Am. Chem. Soc.* **2002**, *124*, 7170.
(16) Tao, F.; Wang, Z. H.; Xu, G. Q. *J. Chem. Phys.* **2001**, *115*, 9563.
(17) Tao, F.; Chen, X. F.; Wang, Z. H.; Xu, G. Q. *J. Phys. Chem. B* **2002**, *106*, 3890.
(18) Tao, F.; Wang, Z. H.; Chen, X. F.; Xu, G. Q. *Phys. Rev. B* **2002**, *65*, art. no. 115311.

(19) Tao, F.; Wang, Z. H.; Xu, G. Q. *J. Phys. Chem. B* **2002**, *106*, 3557.
(20) Tao, F.; Xu, G. Q. *Phys. Rev. B*, **2002**, *66*, art. no. 03546.
(21) Lopinski, G. P.; Fortier, T. M.; Moffatt, D. J.; Wolkow, R. A. *J. Vac. Sci. Technol. A* **1998**, *16*, 1037.
(22) Lopinski, G. P.; Moffatt, D. J.; Wolkow, R. A. *Chem. Phys. Lett.* **1998**, *282*, 305.
(23) Clemen, L.; Wallace, R. M.; Taylor, P. A.; Dresser, M. J.; Choyke, W. J.; Weinberg, W. H.; Yates, J. T., Jr. *Surf. Sci*. **1992**, *268*, 205.
(24) Taguchi, Y.; Fujisawa, M.; Takaokat, T.; Okada, T.; Nishijima, M. *J. Chem. Phys.* **1991**, *95*, 6870.
(25) Lai, P.; Teplyakov, A. V.; Noah, Y. A.; Kong, M. J.; Wang, G. T.; Bent, S. F. *J. Chem. Phys.* **1999**, *110*, 10545.
(26) Hovis, J. S.; Hamers, R. J.; Liu, H. B.; Shan, J. *J. Phys. Chem. B* **1998**, *102*, 687.
(27) Konecny, R.; Doren, D. J. *J. Am. Chem. Soc.* **1997**, *119*, 11098.
(28) Hamers, R. J.; Hovis, J. S.; Lee, S. *J. Phys. Chem. B* **1997**, *101*, 1489.
(29) Teplyakov, A. V.; Lai, P.; Noah, Y. A.; Bent, S. F. *J. Am. Chem. Soc*. **1998**, *120*, 7377.
(30) Yoshinobu, J.; Yamashita, Y.; Tasui, F.; Muki, K.; Akagi, K.; Tsuneyuki, S.; Hamaguchi, K.; Machida, S.; Nagao, M.; Sato, T.; Fwatsuki, M. *J. Electron. Spectrosc.* **2001**, *114*, 389.
(31) Machida, S.; Hamaguchi, K.; Nagao, M.; Yasui, F.; Mukai, K.; Yamashita, Y.; Yoshinobu, J.; Kato, H. S.; Okuyama, H.; Kamawi, M. *J. Phys. Chem. B* **2002**, *106*, 1691.
(32) Nishijima, M.; Yoshinobu, J.; Tsuda, H.; Onchi, M. *Surf. Sci.* **1987**, *192*, 383.
(33) Carbone, M.; Piancastelli, M. N.; Casaletto, M. P.; Ianoni, R.; Comtet, G.; Dujardin, G.; Hellner, L. *Phys. Rev. B* **2000**, *61*, 8531.
(34) Jolly, F.; Bournel, F.; Rochet, F.; Dufour, G.; Sirotti, F.; Taleb, A. *Phys. Rev. B* **1999**, *60*, 2930.
(35) Rochet, F.; Jolly, F.; Bournel, F.; Dufour, G.; Sirotti, F.; Cantin, J. L. *Phys. Rev. B* **1999**, *58*, 11029.
(36) Hovis, J. S.; Hamers, R. J. *J. Phys. Chem.* **1997**, *101*, 9581.
(37) Hovis, J. S.; Liu, H. B.; Hamers, R. J. *J. Phys. Chem. B* **1998**, *102*, 6873.
(38) Teplyakov, A. V.; Kong, M. J.; Bent, S. F. *J. Am. Chem. Soc.* **1997**, *119*, 9, 11100.
(39) Fattal, E.; Radeke, M. R.; Reynolds, G.; Carter, E. A. *J. Phys. Chem. B* **1997**, *101*, 8658.
(40) Wisjaja, Y.; Mysinger, M. M.; Musgrave, C. B. *J. Phys. Chem. B* **2000**, *104*, 2527.
(41) Cao, X.; Coulter, S. K.; Ellison, M. D.; Liu, H.; Liu, J.; Hamers, R. J. *J. Phys. Chem. B* **2001**, *105*, 3759.
(42) Kugler, T.; Thibatu, U.; Abraham, M.; Folkers, G.; Gopel, W. *Surf. Sci.* **1992**, *260*, 64.
(43) Kugler, T.; Ziegler, C.; Gopel, W. *Mater. Sci. Eng. B* **1996**, *37*, 112.
(44) Rummel, R. M.; Ziegler, C. *Surf. Sci.* **1998**, *418*, 303.
(45) Cao, X.; Hamers, R. J. *J. Am. Chem. Soc.* **2001**, *123*, 10988.
(46) Cao, X.; Hamers, R. J. *J. Phys. Chem. B* **2002**, *106*, 1840.
(47) Mui, C.; Wang, G. T.; Bent, S. F.; Musgrave, C. B. *J. Chem. Phys.* **2001**, *114*, 10170.
(48) Mulcahy, C. P. A.; Carman, A. J.; Casey, S. M. *Surf. Sci.* **2000**, *459*, 1.
(49) Tao, F.; Yuan, Z. L.; Chen, X. F.; Wang, Z. H.; Xu, G. Q. *Phys. Rev. B.* in press.
(50) Lu, X.; Xu, X.; Wang, N. Q.; Zhang, Q.; Lin, M. C. *J. Phys. Chem. B* **2001**, *160*, 10069.
(51) Hofer, W. A.; Fisher, A. J.; Lopinski, G. P.; Wolkow, R. A. *Phys. Rev. B* **2001**, *63*, art. no. 085314.
(52) Staufer, M.; Birkenheuer, U.; Belling, T.; Nortemann, F.; Rosch, N.; Widdra, W.; Kpstov, K. L.; Moritz, T.; Menzel, D. *J. Chem. Phys.* **2000**, *112*, 2498.
(53) Qiao, M. H.; Tao, F.; Cao, Y.; Li, Z. H.; Dai, W. L.; Deng, J. F.; Xu, G. Q. *J. Chem. Phys.* **2000**, *104*, 11211.
(54) Tao, F.; Qiao, M. H.; Li, Z. H.; Yang, L.; Dai, Y. J.; Huang, H. G.; Xu, G. Q. *Phys. Rev. B* **2003**, *67*, art. no. 115334.
(55) Moulder, J. F.; Stickle, W. F.; Bomben, K. D. *Handbook of X-ray Photoelectron Spectroscopy*; Perkin-Elmer Corporation: Minnesota, 1992.
(56) *VGX900-Real and Protected Mode Programs*; VG Microtech Ltd.: U.K., 1994.
(57) Cohen, M. R.; Merrill, R. P. *Surf. Sci.* **1991**, *245*, 1.
(58) Qiao, M. H.; Cao, Y.; Deng, J. F.; Xu, G. Q. *Chem. Phys. Lett.* **2000**, *325*, 508.
(59) Liu, H.; Hamers, R. J. *Surf. Sci.* **1998**, *416*, 354.
(60) Bischoff, J. L.; Lutz, F.; Bolmont, D.; Kubler, L. *Surf. Sci*. **1991**, *251/252*, 170.
(61) Dufour, G.; Rochet, F.; Roulet, H.; Sirotti, F. *Surf. Sci.* **1994**, *304*, 33.
(62) Peden, C. H. F.; Rogers, J. W., Jr.; Shinn, N. D.; Kidd, K. B.; Tsang, K. L. *Phys. Rev. B* **1993**, *47*, 15622.
(63) Lindberg, B. J.; Hedman, J. *Chem. Scr.* **1975**, *7*, 155.
(64) Swartz, W. E., Jr.; Gray, R. C.; Carver, J. C.; Taylor, R. C.; Hercules, D. M. *Spectrochim. Acta* **1974**, *30A*, 1561.
(65) Jack, J. J.; Hercules, D. M. *Anal. Chem.* **1971**, *43*, 729.
(66) Long, D. A.; Thomas, E. L. *Trans. Faraday Soc.* **1963**, *59*, 783.
(67) Wiberg, K. B.; Walters, V. A.; Wong, K. N.; Colson, S. D. *J. Phys. Chem.* **1984**, *88*, 6067.
(68) Grassian, V. H.; Mutterties, E. L. *J. Phys. Chem.* **1986**, *90*, 5900.
(69) Cao, Y.; Wei, X. M.; Chin, W. S.; Lai, Y. H.; Deng, J. F.; Bernasek, S. L.; Xu, G. Q. *J. Phys. Chem. B* **1999**, *103*, 5698.
(70) Stidham, H. D. *Spectrochim. Acta* **1965**, *21*, 23.
(71) Hagemann, H.; Bill, H.; Joly, D.; Muller, P.; Pautex, N. *Spectrochim. Acta A* **1985**, *41*, 751.
(72) Carreira, L. A.; Cater, R. O.; Durig, J. R. *J. Chem. Phys.* **1973**, *59*, 812.
(73) *SPARTAN 5.1*; Wave Function Inc.: Irvine, CA, 1998.
(74) Konecny, R.; Doren, D. J. *Surf. Sci.* **1998**, *417*, 169.
(75) Wang, G. T.; Mui, C.; Musgrave, C. B.; Bent, S. F. *J. Phys. Chem. B* **1999**, *103*, 6803.
(76) Wolkow, R. A.; Lopinski, G. P.; Moffatt, D. J. *Surf. Sci.* **1998**, *416*, L1107.
(77) Hofer, W. A.; Fisher, A. J.; Lopinski, G. P.; Wolkow, R. A. *Phys. Rev. B* **2001**, *63*, 5314.
(78) Silvestrelli, P. L.; Ancilotto, F.; Toigo, F. *Phys. Rev. B* **2002**, *62*, 1596.